

NASA Technical Memorandum 100825

# High Frequency Ultrasonic Characterization of Sintered SiC

(NASA-TM-100825) HIGH FREQUENCY ULTRASONIC  
CHARACTERIZATION OF SINTERED SiC (NASA)  
19 p CACL 14D

N88-23985

Unclas  
G3/38 0146039

George Y. Baaklini, Edward R. Generazio, and James D. Kiser  
*Lewis Research Center*  
*Cleveland, Ohio*

Prepared for the  
11th Annual Conference on Composite and Advanced Ceramic Materials  
sponsored by the American Ceramic Society  
Cocoa Beach, Florida, January 18-23, 1987

**NASA**

# HIGH FREQUENCY ULTRASONIC CHARACTERIZATION OF SINTERED SiC

George Y. Baaklini, Edward R. Generazio, and James D. Kiser  
National Aeronautics and Space Administration  
Lewis Research Center  
Cleveland, Ohio 44135

## ABSTRACT

High frequency 60- to 160-MHz ultrasonic nondestructive evaluation was used to characterize variations in density and microstructural constituents of sintered SiC bars. Ultrasonic characterization methods included longitudinal velocity, reflection coefficient, and precise attenuation measurements. The SiC bars were tailored to provide bulk densities ranging from 90 to 98 percent of theoretical, average grain sizes ranging from 3.0 to 12.0  $\mu\text{m}$ , and average pore sizes ranging from 1.5 to 4.0  $\mu\text{m}$ . Velocity correlated with specimen bulk density irrespective of specimen average grain size, average pore size, and average pore orientation. Attenuation coefficient was found to be sensitive to both density and average pore size variations, but was not affected by large differences in average grain size.

## INTRODUCTION

Reliable quantitative ceramic characterization via nondestructive evaluation (NDE) methodologies is being aggressively pursued throughout the ceramic and nondestructive testing communities. It is necessary to develop NDE techniques for characterizing microstructural and morphological factors which ultimately govern the strength, toughness, and dynamic performance of ceramics.<sup>1</sup> This is because reliability assurance of ceramics depends not only on defect detection but also on mechanical strength verification and associated properties which are sensitive to microstructural characteristics. The ability to nondestructively probe the microstructure of a ceramic via ultrasonic

velocity and attenuation is of high interest for in situ monitoring and control of material processing, and for material properties verification of finished products. Hence, pulse-echo ultrasonics, an effective technique for the characterization of the microstructure and density of structural ceramics,<sup>2-6</sup> was chosen for interrogating the sintered SiC system.

Silicon carbides have fine microstructural constituents,<sup>7-10</sup> that is, grains and pores range in size from 1 to 10  $\mu\text{m}$ . High frequency (short wavelength) ultrasound is required for the characterization of these fine ceramics. But high frequency ultrasonic measurements using contact pulse-echo techniques are limited by variations in specimen surface roughness and couplant thickness.<sup>3</sup> In addition, polished ceramic surfaces are costly and impractical. Consequently, there exists a need (1) to determine an acceptable surface roughness for the silicon carbide system where reliable attenuation measurements can be obtained, (2) to define the proper frequency regime for microstructural characterization, and (3) to quantitatively correlate precision ultrasonic measurements with material properties to the extent that they are controlled by microstructural characteristics.

This work will identify an acceptable specimen surface roughness for obtaining reliable high frequency, contact-pulse-echo ultrasonic attenuation measurements. Further, it will quantitatively assess the dependence of ultrasonic attenuation and velocity on the microstructure and density of sintered silicon carbide.

## EXPERIMENTAL

### Sample Preparation

Green test bars were formed by dry pressing -100 mesh  $\alpha$ -SiC powder that contained boron and carbonaceous resin binders in a double-action

tungsten-lined die at a pressure of 120 MPa. These bars were then vacuum sealed in thin-wall latex tubing and cold isopressed at 414 MPa. The green bars were sintered in batches under 0.1 MPa argon pressure at different temperatures for different sintering hold times (Table I). Some sintered specimens were further hot isostatically pressed under 138 MPa argon pressure at various temperatures for different hold times (Table I). These different sintering and hot isostatic pressing conditions were employed in order to "tailor" the densities and microstructures of the different batches. These conditions provided batches with bulk densities ranging from 2.92 to 3.13 g/cm<sup>3</sup>, with average grain sizes ranging from 3.36 to 11.56  $\mu\text{m}$ , and with average pore sizes ranging from 1.60 to 3.82  $\mu\text{m}$ . Table II lists mean pore sizes, mean grain sizes, and their corresponding shapes for all eight batches. All bars were machined, with the four long edges beveled. These specimens were further polished to 0.45, 0.36, 0.11, and 0.07  $\mu\text{m}$  rms surface finishes. Nominal test bar dimensions were 0.27 by 0.56 by 3.17 cm.

### Microstructural Characterization

Mean pore size, shape, and orientation were determined from photomicrographs of a polished representative sample from each batch by applying two-dimensional Fourier transform theory.<sup>11</sup> Briefly, nine different microstructural images from different areas on the same sample were digitally recorded into a 512 by 512 pixel array via a vidicon camera connected to a video digitizer. The pore boundaries were enhanced by two dimensional digital gradient<sup>12</sup> of the image. All pixels between pores were set to a zero value while pixels belonging to pores were set to a constant nonzero value. Next, a tone-pulse-encoded image containing the fundamental harmonics of each pore was generated in all directions (0 to  $2\pi$  rad). The tone pulse had a width equal

to the width of the pore. Tone-pulse-encoded images were digitally Fourier transformed by using a complex 512 point, hardwired, fast Fourier transform array processor. This enabled the determination of the density of frequency components, from which the density of length components were determined. The latter corresponds directly to the two-dimensional pore size distribution function from which the mean pore size, shape, and orientation are obtained.<sup>11</sup> Figure 1 shows the pore size distribution function (Fig. 1(a)), the mean pore size, shape, and orientation (Fig. 1(b)), and the polished microstructure (Fig. 1(c)) for batch 2.

Mean grain size was determined from photomicrographs of a polished and etched representative sample of each batch by using an interactive image analysis computer system. The computer system is designed for data acquisition and computation of geometric characteristics. By tracing grain boundaries on a digitizing tablet, grain sizes were measured and mean grain sizes were determined for all batches.

#### Ultrasonic Evaluation

Figure 2 shows a typical configuration of the pulse-echo technique which was used for the ultrasonic measurements. Reproducible velocity and attenuation measurements were performed on all samples, through the thickness of each specimen at different locations. The pulse-echo technique, with a 100 MHz broadband longitudinal-wave transducer, was used to measure the cross correlation velocity<sup>13</sup> and the attenuation coefficient<sup>3</sup> from the first and second back surface reflections. The frequency dependent reflection coefficient was incorporated for precision attenuation measurements. A valid frequency zone was defined between 60 and 160 MHz outside of which the reflection coefficient is subject to large errors.

The reflection coefficient of the buffer rod-couplant-sample (BCS) interface as a function of frequency,  $f$ , for a specific surface roughness can be determined from the ratio of the magnitude of the Fourier spectra of the front surface reflection with the sample present on the buffer rod,  $|FS_2(f)|$ , to that of the front surface reflection without the sample present on the buffer rod,  $|FS_1(f)|$

$$|R(f)| = \frac{|FS_2(f)|}{|FS_1(f)|} \quad (1)$$

The frequency dependent attenuation coefficient can be determined from the Fourier magnitudes of the first and second back-surface reflections,  $|B_1(f)|$  and  $|B_2(f)|$ , respectively and is given by<sup>3</sup>

$$\alpha(f) = \frac{1}{2 \Delta X} \ln \left\{ \frac{|B_1(f)| |R(f)|}{|B_2(f)|} \right\} \quad (2)$$

where  $\Delta X$  is the thickness of the sample.

## RESULTS AND DISCUSSION

### Reflection Coefficient and Surface Roughness

The experimentally determined reflection coefficients as a function of frequency for machined and polished specimens were obtained by using Eq. (1). Figure 3 shows experimental reflection coefficients for a typical SiC sample at varying surface roughness. A decrease in the surface roughness leads to a decrease in the couplant thickness. This results in a decrease in the reflection coefficient to approach the theoretical value of the zero frequency reflection coefficient  $|R(0)|$  given by

$$|R(0)| = \left| \frac{Z_3 - Z_1}{Z_3 + Z_1} \right| \quad (3)$$

where  $Z_1$  and  $Z_3$  are the acoustical impedance of the buffer rod and sample, respectively.

Figure 4 shows that the reflection coefficient is an increasing function of the maximum peak-to-valley roughness  $R_t$  at a fixed frequency. It also shows that samples with different densities may yield similar reflection coefficient values for different maximum peak-to-valley roughnesses. This difference in roughness will change the effective couplant thickness and the contact area between the sample and the buffer rod surface. In addition, it may include other topological variations, related to that specific batch or sample, which scatter energy out of the main pulse in a random manner. Polishing sintered silicon carbide samples down to a surface roughness of  $0.11 \mu\text{m rms}$  is necessary to approach the theoretical zero frequency reflection coefficients for the batches used here. However, it is still necessary to incorporate the frequency dependent reflection coefficient in the ultrasonic attenuation measurements in order to improve the accuracy of these measurements.<sup>3</sup>

#### Attenuation Coefficient and Microstructural Variations

The attenuation coefficient as a function of frequency for each sample was obtained by using Eq. (2) where the frequency dependent reflection coefficient was incorporated. Figure 5 shows the attenuation coefficient measurements for varying surface roughness of the same sample that was considered in Fig. 3. It is noted that for surface roughness less than or equal to  $0.11 \mu\text{m rms}$  attenuation measurements (Fig. 5) become less dependent on the surface roughness in the frequency regime shown. In addition, Fig. 6

shows the actual percent uncertainty of the measured attenuation coefficient due to the uncertainty in the pulse amplitudes. The actual percent uncertainty was calculated by using Eq. (4) below<sup>3</sup>

$$\left| \frac{\sigma_{\alpha}}{\alpha} \right| (100) = \frac{1}{2\alpha \Delta X} \left( \frac{100}{(s/n)} \right) \left[ \left( \frac{(\exp(2\alpha \Delta X) + |R|^2) \exp(2\alpha \Delta X)}{(1 - |R|^2)^2} + 1 \right) \frac{1}{|R|^2 + 1} + 1 \right]^{1/2} \quad (4)$$

where  $\sigma_{\alpha}$  is the variance of the attenuation, and  $s/n$  is the signal-to-noise ratio of the main pulse  $FS_1(f)$ . For varying surface roughness the percent uncertainty is less than 5 percent, except when the attenuation approaches zero, here the percent uncertainty increases dramatically. Hence polishing sintered silicon carbide samples down to a surface roughness of less than or equal to 0.11  $\mu\text{m}$  rms is necessary to obtain accurate comparative attenuation measurements for samples from different batches.

Attenuation coefficient results are plotted as a function of frequency for all batches in Fig. 7. Solid lines represent the upper and lower boundaries of the data for each batch (1, 4, and 5HP) of specimens. The data for batches 2, 2HP, 3, 3HP, and 4HP were spread and overlapped between the two solid lines as indicated by the arrows in Fig. 7, making it difficult to clearly show all the data separately for each batch. At 100 MHz the attenuation coefficient does differentiate substantially between batches, on the basis of their density and microstructural constituents. The attenuation and microstructural data for batches 1, 4, and 5HP does not show clear evidence of the attenuation dependence on one single scattering mechanism. But from attenuation data<sup>14</sup> measured on the same silicon carbide system, it was found that attenuation was not due to grain boundary scattering. Hence,



pore site scattering is the dominant attenuation mechanism. Attenuation due to pore site scattering depends mainly on the average pore size and the porosity distribution (density).

Attenuation dependency on average pore size can be seen by comparing batch 1 and batch 4HP (with a similar density) attenuation coefficient data shown in Fig. 8. For an average pore size increase of ~115 percent the mean attenuation coefficient increased by 300 percent at 100 MHz.

Attenuation dependency on density can be demonstrated by comparing batch 4 and batch 4HP attenuation coefficient data shown in Fig. 8. An ~1.97 percent increase in density reflects a 150 percent decrease in mean attenuation coefficient at 100 MHz.

#### Velocity and Density

The average ultrasonic velocity through the SiC bars was plotted as a function of specimen bulk density in Fig. 9(a). The average velocity for each of batch 1, 2, 2HP, 3, 3HP, 4, 4HP, and 5HP are 1.181, 1.175, 1.186, 1.186, 1.176, 1.190, 1.160, 1.188, and 1.101 cm/ $\mu$ sec, respectively. The data show that velocity is an increasing function of bulk density. This result agrees with previous findings.<sup>5-6</sup>

Figure 9(b) shows the velocity data for batches 1, 4, 4HP, and 5HP. Velocity was not as sensitive to changes in mean grain and pore size as it was to changes in bulk density, that is, no substantial difference in velocity was detected between batch 4HP (1.188 cm/ $\mu$ s) and batch 1 (1.181 cm/ $\mu$ s), each of which had average densities of 3.11 g/cm<sup>3</sup>, even though 4HP had more than twice the mean grain and pore size of batch 1.

Velocity was not sensitive to preferred mean pore orientation for batches with identical densities and with roughly close average pore and grain sizes

(Fig. 9(c)). In the case of batch 2 the major axis of the mean pore (Fig. 1) was perpendicular to the sound propagation direction, whereas the mean pore in batch 3 had its major axis parallel to the sound of propagation.

#### GENERAL DISCUSSION

Attenuation measurement, although sensitive to the surface roughness of silicon carbide ceramics, is an excellent indicator of porosity variations between specimens. Further, for a polished system (surface roughness less than or equal to  $0.11 \mu\text{m rms}$ ) where porosity is the main ultrasonic scattering mechanism (assuming similar average pore size), attenuation measurement is a more sensitive indicator than velocity measurement in detecting and monitoring density differences. For example, by comparing the data for batch 4 and 4HP, a 1.97 percent increase in density was characterized by a 150 percent decrease in mean attenuation coefficient at 100 MHz as opposed to a 1.7 percent increase in average velocity.

Velocity measurement, which is less sensitive to microstructural variations, is an attractive indicator of density variations in machined or polished ceramics. Especially, when both density and mean pore size are changing at the same time (general case).

For ceramic batches with very fine microstructural constituents and near full theoretical density (similar to or of better quality than batch 1), higher frequency regimes (up to 300 MHz) need to be considered for attenuation measurements to detect porosity variations between specimens and or batches. Such fine hot isostatically pressed SiC has recently been developed.<sup>15</sup> In addition, sintered silicon nitride materials in general have microstructures that are up to one order of magnitude finer<sup>16</sup> than silicon carbides.

## CONCLUSIONS

Surface roughness constraints on comparative and precise attenuation measurements have been identified for the sintered SiC system. A surface roughness of  $0.11 \mu\text{m rms}$  is required for accurate ultrasonic attenuation measurements. Ultrasonic longitudinal velocity correlated well with specimen bulk densities. Velocity was not found to be sensitive to average grain size, average pore size, and average pore orientation. Velocity measurement is an attractive ultrasonic parameter for monitoring and evaluating the density of machined or polished ceramics. Precise attenuation measurements, which are sensitive to variations in surface roughness, were obtained by incorporating the frequency dependent reflection coefficient in the signal analysis. These measurements are found to be extremely sensitive to density and average pore size. When porosity is the only scattering mechanism that affects attenuation measurements, the latter is expected to present a much higher sensitivity than velocity measurements in detecting minute density variations.

## REFERENCES

- <sup>1</sup>Vary, A., "Quantitative Ultrasonic Evaluation of Engineering Properties in Metals, Composites, and Ceramics"; NASA TM-81530, June 1980.
- <sup>2</sup>Evans, A.G., et al, "Ultrasonic Attenuation in Ceramics," J. Appl. Phys. **49** [5], pp. 2669-2679 May 1978.
- <sup>3</sup>Generazio, E.R., "The Role of the Reflection Coefficient in Precision Measurement of Ultrasonic Attenuation," Mater. Eval. **43** [8], 995-1004 (1985).
- <sup>4</sup>Kupperman, D.S., "Application of NDE Methods to Green Ceramics: Initial Results," ANL/FE-83-25, March 1984.
- <sup>5</sup>S.J.Klima, and G.Y.Baaklini, "Nondestructive Characterization of Structural Ceramics," SAMPE Q. **17** [3], April (1986).
- <sup>6</sup>Thorp, J.S., and Bushell, T.G., "Ultrasonic Examination of Reaction Bonded Silicon Nitride," J. Mater. Sci. **20**, 2265-2274, 1985.
- <sup>7</sup>Dutta, S., "Sinterability, Strength and Oxidation of Alpha Silicon Carbide Powders," Journal of Materials Science **19**, 1307-1313, 1984.
- <sup>8</sup>Dutta, S., "Strength Optimization of  $\alpha$ -SiC by Improved Processing," NASA CP 2427, pp. 89-98, May 1986.

- <sup>9</sup>Hurst, J.B., and Millard, M.L., "Evaluation of a-SiC Sintering Using Statistical Methods," J. Am. Ceram. Soc. 68 [7] C-1782181, July 1985.
- <sup>10</sup>Helms, H.E., et al, "Ceramic Materials Development," pp. 49-63 in Ceramic Applications in Turbine Engines, Noyes Publications, Park Ridge, NJ, 1986.
- <sup>11</sup>Generazio, E.R., "Determination of Grain Size Distribution Function Using Two-Dimensional Fourier Transforms of Tone Pulse Encoded Images," Mater. Eval., 46 [4] 528-534 (1988).
- <sup>12</sup>Gonzalez, R.C., and Wintz, P., Digital Image Processing, 1977, Addison-Wesley, Reading, MA, 1977.
- <sup>13</sup>Hull, D.R., Kautz, H.E., and Vary, A., "Measurement of Ultrasonic Velocity Using Phase-Slope and Cross Correlation Methods," Mater. Eval., 43 [11] 1455-1460 (1985).
- <sup>14</sup>Generazio, E.R., Roth, D.J., and Baaklini, G.Y., "Imaging Subtle Microstructural Variations in Ceramics with Precision Ultrasonic Velocity and Attenuation Measurements," NASA TM-100129, November 1987.
- <sup>15</sup>Dutta, S., "Improved Processing of a-SiC", Adv. Ceram. Mater., 1988.

<sup>16</sup>Sanders, W.A., and Baaklini, G.Y., "Correlation of Processing and Sintering Variables with the Strength and Radiography of Silicon Nitride," Adv. Ceram. Mater. 3 [1] 88-94 1988.

TABLE I. - SINTERING AND HOT ISOSTATIC PRESSING CONDITIONS

Batch number	Number of specimen	Sintering			Hot isostatic pressing			Density, g/cm <sup>3</sup> ± 0.01 g/cm <sup>3</sup>
		Temperature, °C	Time, hr	Argon pressure, MPa	Temperature, °C	Time, hr	Argon pressure, MPa	
1	10	2200	0.5	0.1	----	---	---	3.11
2	10	2200	1.5	↓	----	---	---	3.09
2HP	7	2200	1.5		2100	0.5	138	3.13
3	9	2150	4.0		----	---	---	3.09
3HP	9	2150	4.0		2100	0.5	138	3.12
4	8	2300	1.0		----	---	---	3.05
4HP	8	2300	1.0	2150	1.0	138	3.11	
5HP	9	2100	.75	↓	2100	1.0	138	2.92

TABLE II. - CHARACTERIZATION OF MICROSTRUCTURE

Batch number	Density, g/cm <sup>3</sup>	Mean grain size, <sup>a</sup> μm			Grain shape	Mean pore size, <sup>a</sup> μm			Pore orientation
		Circle <sup>b</sup>		Ellipse <sup>c</sup>		Circle <sup>d</sup>		Ellipse <sup>a,e</sup>	
		Diameter	Major	Minor		Diameter	Major	Minor	
1	3.11	5.76	7.94	4.56	Equiaxed and elongated	1.60	1.61	1.59	-----
2	3.09	5.38	7.52	4.20	Equiaxed and elongated	1.61	1.90	1.31	Preferred
2HP	3.13	6.75	9.61	5.15	Equiaxed and elongated	1.63	1.75	1.50	-----
3	3.09	4.13	5.39	3.38	Equiaxed and elongated	1.82	2.04	1.59	Preferred
3HP	3.12	4.04	5.24	3.36	Equiaxed but few elongated	1.68	1.75	1.61	-----
4	3.05	11.56	19.39	7.73	Elongated	3.82	4.00	3.64	-----
4HP	3.11	11.18	18.08	7.82	Elongated	3.44	3.60	3.27	-----
5HP	2.92	3.36	4.40	2.78	Equiaxed	2.29	2.38	2.19	-----

<sup>a</sup>±0.2 μm.

<sup>b</sup>Assuming all grains are equiaxed.

<sup>c</sup>Assuming all grains are elongated.

<sup>d</sup>Calculated average from e.

<sup>e</sup>Real measurements off the mean shape.

ORIGINAL PAGE IS  
OF POOR QUALITY

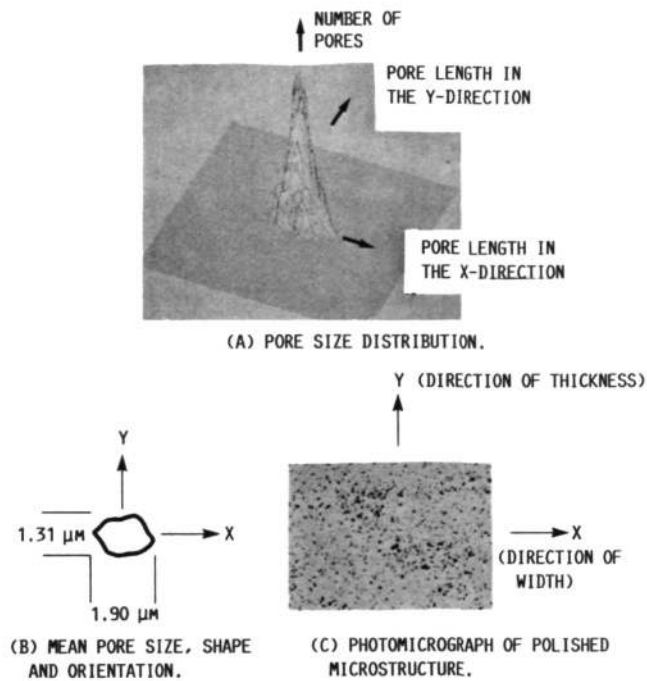


FIGURE 1. POROSITY CHARACTERIZATION OF A POLISHED SAMPLE FROM BATCH 2.

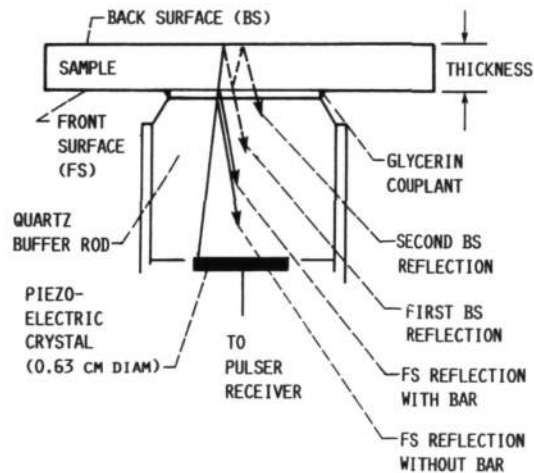


FIGURE 2. - PULSE-ECHO ULTRASONICS OF SiC BARS.

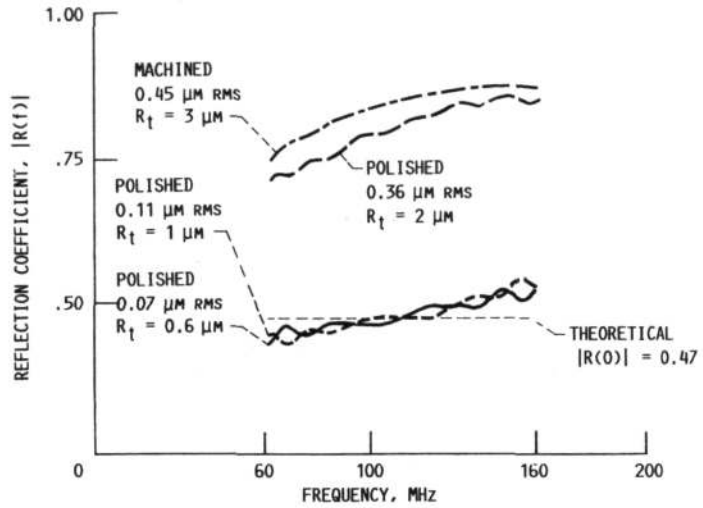


FIGURE 3. - REFLECTION COEFFICIENT FOR VARYING SURFACE ROUGHNESS OF THE SAME SAMPLE.  $R_t$  IS MAXIMUM PEAK-TO-VALLEY HEIGHT.  $R(0)$  IS THE THEORETICAL REFLECTION COEFFICIENT AT ZERO FREQUENCY.

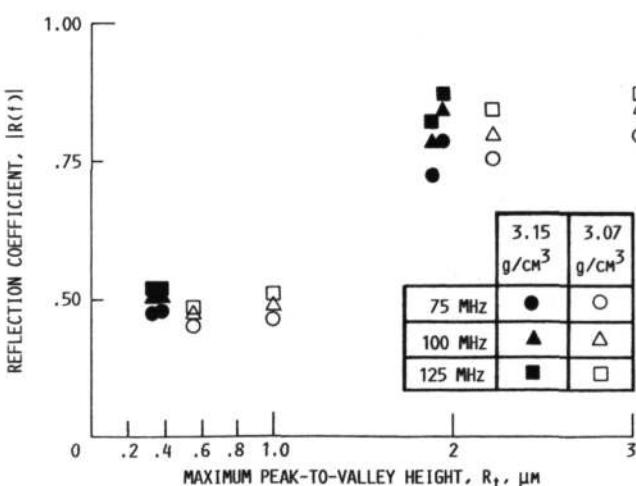


FIGURE 4. - REFLECTION COEFFICIENT VERSUS MAXIMUM PEAK-TO-VALLEY HEIGHT.

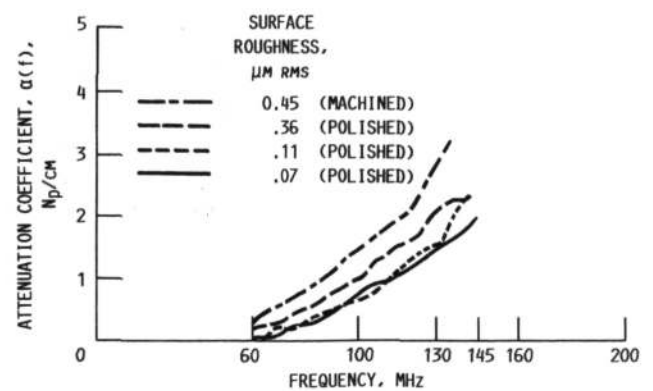


FIGURE 5. - ATTENUATION COEFFICIENT MEASUREMENTS FOR VARYING SURFACE ROUGHNESS OF THE SAME SAMPLE.



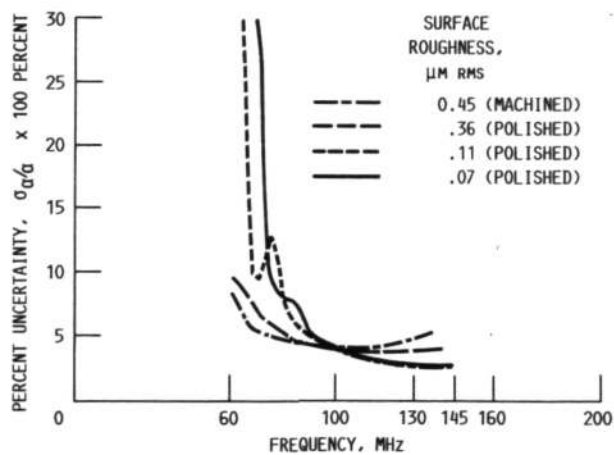


FIGURE 6. - UNCERTAINTY IN THE MEASURED ATTENUATION COEFFICIENT FOR VARYING SURFACE ROUGHNESS OF THE SAME SAMPLE.

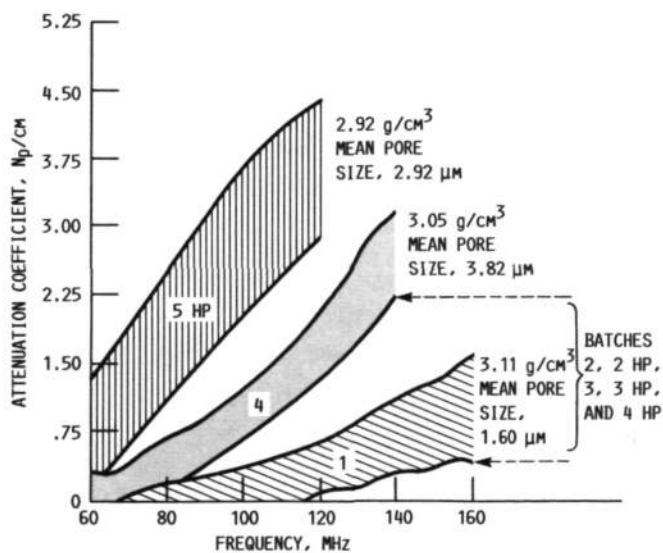


FIGURE 7. - ATTENUATION COEFFICIENT AS A FUNCTION OF FREQUENCY FOR SiC BATCHES WITH DIFFERENT DENSITIES AND MICROSTRUCTURES.

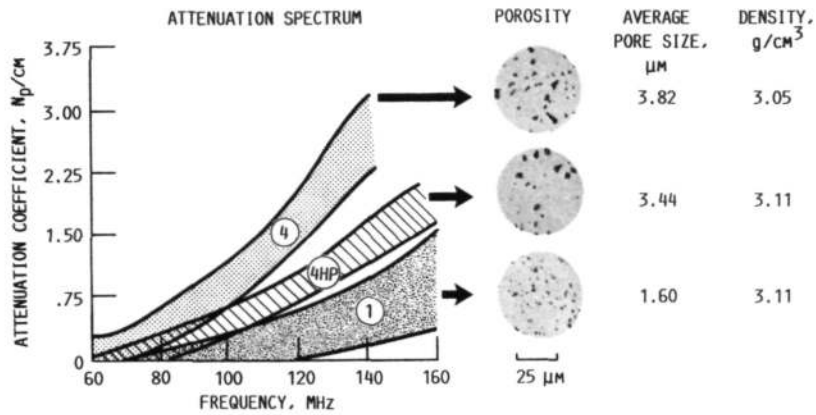


FIGURE 8. - ATTENUATION COEFFICIENT AS A FUNCTION OF FREQUENCY FOR BATCHES 1, 4, AND 4 HP.

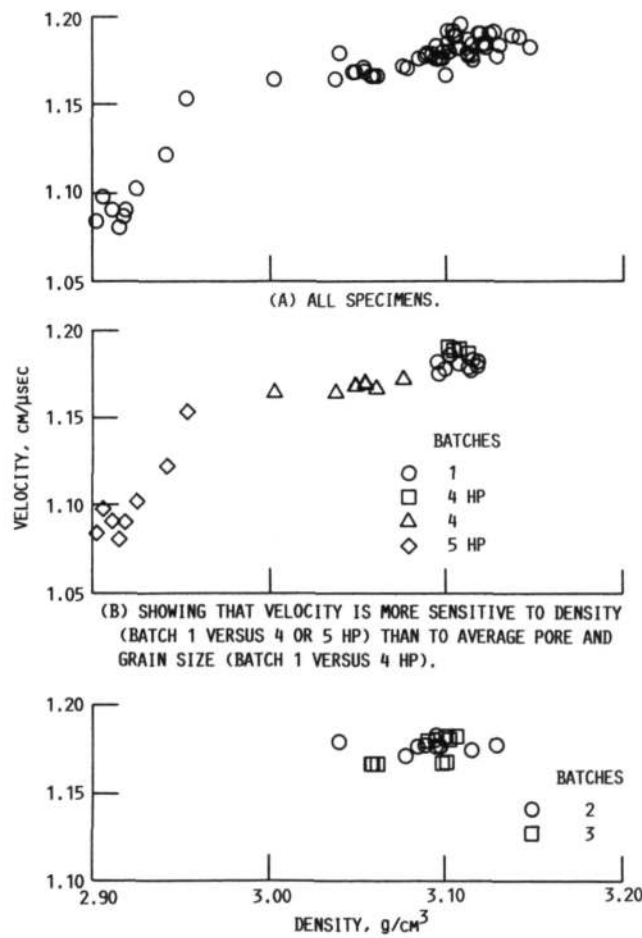


FIGURE 9. - ULTRASONIC VELOCITY AS A FUNCTION OF SPECIMEN BULK DENSITY.

1. Report No. NASA TM-100825		2. Government Accession No.		3. Recipient's Catalog No.	
4. Title and Subtitle High Frequency Ultrasonic Characterization of Sintered SiC				5. Report Date	
				6. Performing Organization Code	
7. Author(s) George Y. Baaklini, Edward R. Generazio, and James D. Kiser				8. Performing Organization Report No. E-4013	
				10. Work Unit No. 533-07-01	
9. Performing Organization Name and Address National Aeronautics and Space Administration Lewis Research Center Cleveland, Ohio 44135-3191				11. Contract or Grant No.	
				13. Type of Report and Period Covered Technical Memorandum	
12. Sponsoring Agency Name and Address National Aeronautics and Space Administration Washington, D.C. 20546-0001				14. Sponsoring Agency Code	
15. Supplementary Notes Prepared for the 11th Annual Conference on Composite and Advanced Ceramic Materials sponsored by the American Ceramic Society, Cocoa Beach, Florida, January 18-23, 1987.					
16. Abstract  High frequency 60- to 160-MHz ultrasonic nondestructive evaluation was used to characterize variations in density and microstructural constituents of sintered SiC bars. Ultrasonic characterization methods included longitudinal velocity, reflection coefficient, and precise attenuation measurements. The SiC bars were tailored to provide bulk densities ranging from 90 to 98 percent of theoretical, average grain sizes ranging from 3.0 to 12.0 $\mu\text{m}$ , and average pore sizes ranging from 1.5 to 4.0 $\mu\text{m}$ . Velocity correlated with specimen bulk density irrespective of specimen average grain size, average pore size, and average pore orientation. Attenuation coefficient was found to be sensitive to both density and average pore size variations, but was not affected by large differences in average grain size.					
17. Key Words (Suggested by Author(s)) Ultrasonics; High frequency; Ceramics; Nondestructive testing/evaluation; Velocity; Attenuation; Microstructural characterization; Sintered SiC			18. Distribution Statement Unclassified - Unlimited Subject Category 38		
19. Security Classif. (of this report) Unclassified		20. Security Classif. (of this page) Unclassified		21. No of pages 18	22. Price* A02

National Aeronautics and  
Space Administration

Lewis Research Center  
Cleveland, Ohio 44135

Official Business  
Penalty for Private Use \$300

FOURTH CLASS MAIL

ADDRESS CORRECTION REQUESTED



Postage and Fees Paid  
National Aeronautics and  
Space Administration  
NASA-451

**NASA**

---